The Shape Awakens: Estimating Dynamic Soft Robot States from the Outer Rim

Tongjia Zheng and Jessica Burgner-Kahrs

***Abstract*— State estimation for soft continuum robots is challenging due to their infinite-dimensional states (poses, strains, velocities) resulting from continuous deformability, while conventional sensors provide only discrete data. A recent method, called a boundary observer, uses Cosserat rod theory to estimate all robot states by measuring only tip velocity. In this work, we propose a novel boundary observer that instead measures the internal wrench at the robot's base, leveraging the duality between velocity and internal wrench. Both observers are inspired by energy dissipation, but the base-based approach offers a key advantage: it uses only a 6-axis force/torque sensor at the base, avoiding the need for external sensing systems. Combining tip- and base-based methods further enhances energy dissipation, speeds up convergence, and improves estimation accuracy. We validate the proposed algorithms in experiments where all boundary observers converge to the ground truth within 3 seconds, even with large initial deviations, and they recover from unknown disturbances while effectively tracking high-frequency vibrations.**

I. Introduction

Accurate state estimation is essential for effective control and operation of robots. For continuum robots, this is particularly challenging because their states are inherently *infinite-dimensional* functions due to the robots' continuous deformability. As traditional sensing techniques only provide discrete measurements, one common strategy is to combine with mathematical models to infer unmeasured continuous states. Most existing research has focused on quasi-static shape estimation, ranging from fitting parameterized spatial curves [1], [2] to applying Kalman filters based on Kirchhoff rod statics [3] and employing Gaussian process regression for Cosserat rod statics [4]. Shape estimation, however, is unsuitable for real-time dynamic control. Consequently, there is a shift towards incorporating dynamic models. Cosserat rod theory is perhaps the most widely adopted [5]–[7]. However, it leads to nonlinear partial differential equations (PDEs), making state estimation particularly challenging. Researchers have developed various discretized or reduced-order models, such as finite difference [8], piecewise constant curvature [9], piecewise constant strain [10], and smooth strain parameterizations [11]. Using these discretized or reduced-order models, techniques like extended Kalman filters [12], [13], passivity-based observers [8], and state-dependent Kalman filters [14] have been designed. The common limitation is that they often require a large number of measurements and cannot guarantee the convergence of estimates. This raises a fundamental question: *Are the infinite-dimensional robot states observable based on current sensing techniques?*

Continuum Robotics Laboratory, University of Toronto, ON, Canada. (tongjia.zheng@utoronto.ca, jessica.burgnerkahrs@utoronto.ca)

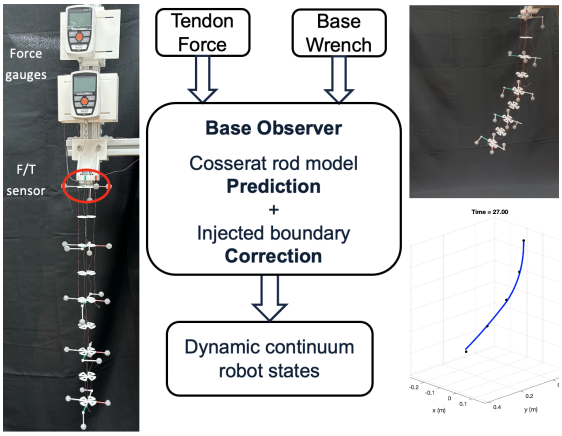

Fig. 1. Overview. Our algorithm estimates dynamic robot states by integrating the Cosserat rod model with tendon forces and an injected correction based on the measured internal wrench at the robot's base. Left: experimental setup. Middle: flowchart of our algorithm. Right: state estimates converge to the ground truth.

Recently, a dynamic state estimation method called a boundary observer was introduced [15], [16], which employs Cosserat rod theory to recover all infinite-dimensional states by measuring only the velocity twist at the robot's tip. We refer to this method as the *tip observer*. In this work, we propose a dual boundary observer—the *base observer*—that also reconstructs the full dynamic state but instead relies on measurements of the internal wrench at the robot's base. This design leverages the duality between velocity and internal wrench, with both observers grounded in energy dissipation principles. Despite their mathematical duality, the base observer offers a practical advantage: it requires only a 6-axis force/torque (F/T) sensor at the base, making it suited for small-scale continuum robots and for applications such as inspection in outdoor or constrained environments. Moreover, combining tip- and base-based correction techniques enhances energy dissipation, speeds up convergence, and improves estimation accuracy—making the integrated approach especially valuable when both types of sensing are available. Experimental validation using a tendon-driven continuum robot shows that all boundary observers converge to the ground truth within 3 seconds, even from significantly deviated initial conditions. They also recover from unknown disturbances and accurately track high-frequency vibrations. Furthermore, combining the correction mechanisms leads to faster convergence and higher accuracy. Implemented in MATLAB and executed at 30 Hz, the algorithm achieves a real-time factor of 1.52 ± 0.33, confirming its suitability for real-time control applications. An overview of the experimental results is shown in Figure 1.

II. Dissipation-Based Boundary Observers

Our state estimation algorithm is based on the Cosserat rod theory [6], [7]. The robot states are continuous functions of the arc parameter $s \in [0,1]$ and time t. Let $g(s,t) \in SE(3)$ be the field of poses (transformation matrices) of the robot. Let $\eta(s,t), \xi(s,t), \phi(s,t), \psi(s,t) \in \mathbb{R}^6$ be the fields of velocity twists, strain twists, internal wrenches, and external wrenches, respectively. The governing equations of robot kinematics and dynamics are given by:

$$\xi_t = \eta_s + \mathrm{ad}_\xi \eta, \tag{1}$$

$$M\eta_t - \mathrm{ad}_\eta^T M\eta = \phi_s - \mathrm{ad}_\xi^T \phi + \psi, \tag{2}$$

with supplementary equations to construct g and ϕ:

$$g_s = g\xi^\wedge, \tag{3}$$

$$\phi = K(\xi - \xi_o) - \phi_{\text{act}}, \tag{4}$$

where $(\cdot)_t$ and $(\cdot)_s$ are partial derivatives, $M(s), K(s) \in \mathbb{R}^{6\times 6}$ are the cross-sectional inertia and stiffness matrices, $\xi_o(s) \in \mathbb{R}^6$ is the reference strain field, and $\phi_{\text{act}}(s,t)$ is the actuation wrench determined by the applied tendon forces $\tau_i(t)$ [17]. Finally, we have the following boundary conditions at $s = 0$ (the base) and $s = 1$ (the tip):

$$g(0,t) = g_0(t), \eta(0,t) = \eta_0(t), \phi(1,t) = \psi_1(t), \tag{5}$$

where $g_0(t)$ is the base pose, $\eta_0(t)$ is the base velocity twist, and $\psi_1(t)$ is the wrench applied at the tip.

Problem Statement: Assume the coefficients $M(s)$ and $K(s)$, the boundary conditions $g_0(t)$, $\eta_0(t)$, and $\psi_1(t)$, the external wrench $\psi(s,t)$, and the tendon inputs $\tau_i(t)$ are known. Assume we can measure the internal wrench at the base $\bar{\phi}(t)$. The objective is to estimate the continuum robot states $g(s,t)$, $\xi(s,t)$, $\eta(s,t)$, and $\phi(s,t)$. This setup is advantageous as it eliminates the need for external sensing systems like motion capture cameras.

Our base observer algorithm is inspired by the principle of energy dissipation. The core equations consist of (1)-(4), which essentially mirror those of the Cosserat rod theory. The novelty lies in the modified boundary conditions:

$$g(0,t) = g_0(t), \tag{6}$$

$$\eta(0,t) = \eta_0(t) + \Gamma_0\big(\phi(0,t) - \bar{\phi}(t)\big), \tag{7}$$

$$\phi(1,t) = \psi_1(t), \tag{8}$$

where $\phi(0,t)$ is the current estimate of the base internal wrench, and $\bar{\phi}(t)$ is the measured internal wrench from a 6-axis F/T sensor. Numerically solving the base observer yields all state estimates. This base observer contrasts with the tip observer in [15], [16], differing only in the boundary conditions. The convergence can be proven using a similar Lyapunov-based methodology in [16], which is essentially a duality property. For completeness, we also present the boundary conditions of the tip observer:

$$g(0,t) = g_0(t), \tag{9}$$

$$\eta(0,t) = \eta_0(t), \tag{10}$$

$$\phi(1,t) = \psi_1(t) - \Gamma_1\big(\eta(1,t) - \bar{\eta}(t)\big), \tag{11}$$

where $\eta(1,t)$ is the current estimate of the tip velocity and $\bar{\eta}(t)$ is the measured tip velocity.

The added terms $\Gamma_0\big(\phi(0,t) - \bar{\phi}(t)\big)$ and $-\Gamma_1\big(\eta(1,t) - \bar{\eta}(t)\big)$ are referred to as *boundary correction terms*. The first acts as a virtual swinging base, and the second as a virtual damping wrench at the tip. It is important to note that these correction terms dissipate the energy associated with the estimation errors rather than the actual robot system. By subtracting the equations for the estimated states from those of the actual robot, one can see that the correction terms act as dissipative terms in the error dynamics.

In fact, the tip and base observers are "additive", enabling their combined use to improve convergence speed, although this comes at the cost of requiring more sensors. The most general boundary conditions of a boundary observer, combining both base and tip corrections, are given by:

$$g(0,t) = g_0(t), \tag{12}$$

$$\eta(0,t) = \eta_0(t) + \Gamma_0\big(\phi(0,t) - \bar{\phi}(t)\big), \tag{13}$$

$$\begin{aligned}\phi(1,t) = \psi_1(t) &- \Gamma_{\text{P}}\big[\log\big(\bar{g}^{-1}(t)g(1,t)\big)\big]^\vee \\ &- \Gamma_{\text{D}}\big(\eta(1,t) - \bar{\eta}(t)\big),\end{aligned} \tag{14}$$

where $g(1,t)$ denotes the estimated tip pose, $\bar{g}(t)$ is the measured tip pose, and Γ_{P}, Γ_{D} are positive-definite gain matrices. The subscripts "P" and "D" reflect their roles akin to proportional-derivative control. Depending on the presence of the P term, we refer to the corresponding observer as the *tip D observer* or *tip PD observer*. These observers offer several key advantages: (1) they can be initialized from any reasonable configuration, with the correction terms ensuring convergence of the estimation errors; and (2) they are compatible with any numerical solver for Cosserat rod models, since the observers remain governed by the same equations. This latter property is particularly beneficial, as the growing popularity of Cosserat rod theory continues to drive the development of efficient solvers, all of which can be readily used to implement the boundary observers.

As model-based algorithms, the accuracy of these observers relies on the fidelity of the underlying model. In the presence of modeling errors, the observers remain stable, though steady-state estimation errors may arise. However, the proportional term helps mitigate these errors by introducing corrective inputs, a property that will be demonstrated through experimental validation.

III. Experimental Validation

In this section, we describe the physical continuum robot and the experimental procedures used to evaluate the performance of the proposed boundary observers.

1) Experimental Setup: The robot features a spring steel rod backbone with nine equally spaced disks. A 6-axis force/torque sensor is mounted at the base to measure internal wrenches in real time. Actuation is achieved using two parallel tendons, each connected to a force gauge at the base to monitor tendon tension. To establish a ground truth for the robot's state, markers were placed on five equally spaced disks and tracked using a motion capture system. The robot

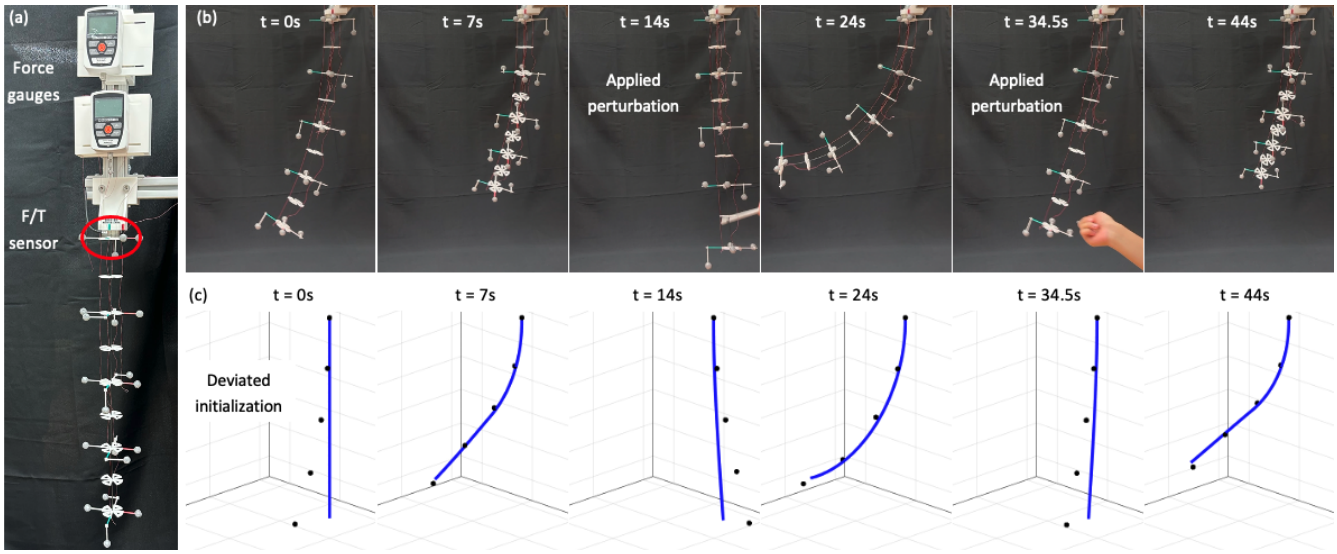

Fig. 2. (a) Experimental Setup: The robot was actuated by two parallel tendons. Tracking markers were placed on five spacer disks to measure their position and orientation, serving as ground truth. A 6-axis F/T sensor was mounted at the robot's base to measure its real-time internal wrenches, while a force gauge was attached to each tendon to record its real-time tension. (b) Experimental Snapshots: The two tendons were pulled to generate spatial motions. At $t = 13.5$ and 34 seconds, external perturbations were applied to the robot to induce high-frequency free vibrations. (c) Estimated Configuration for Corresponding Snapshots: The black dots represent the ground truth positions of the robot's backbone, while the blue curve denotes the estimated backbone position obtained using the base observer algorithm. At $t = 0$, the algorithm was deliberately initialized when the robot was already in motion, resulting in a large initial estimation error. However, the estimated positions quickly converged to the ground truth and closely tracked the robot's actual motion. Upon perturbation, the estimation temporarily deviated from the ground truth but rapidly converged again.

was initially at rest in a vertically downward configuration. To induce diverse spatial motions, we alternated pulling the two tendons. External perturbations were introduced at $t = 13.5$ and 34 seconds by stirring the robot's tip with a stick, generating free vibrations. These conditions were designed to test the observers' ability to recover from unknown disturbances and accurately estimate dynamic states during fast motions, scenarios that violate the quasi-static assumption. A sequence of experimental snapshots is presented in Fig. 2 (b).

2) Experimental Results: In Fig.2, we show the ground truth backbone positions alongside the estimated configurations obtained using the base observer across six experimental snapshots. Due to space constraints, Fig.3 presents only the position and linear velocity trajectories at the three-quarter point of the robot, comparing ground truth and observer estimates. As shown, all observers converged within 2 seconds after initialization, though with varying steady-state errors. The tip PD and combined observers achieved smaller steady-state errors, thanks to the proportional correction term. Initial velocity overshoots, primarily caused by large initialization errors, can be reduced by initializing the observers closer to the true robot state. At $t = 13.5$ and 34 seconds, the base and tip D observers temporarily deviated due to external perturbations but recovered within 1 second and accurately captured high-frequency vibrations. In contrast, the tip PD and combined observers maintained better tracking performance even during disturbances. These results highlight the strengths of our dynamic state estimation framework over quasi-static approaches. Among all observers, the combined observer consistently achieved the fastest convergence and least oscillation, benefiting from the synergy of multiple dissipation-based correction terms.

Finally, all experiments were performed on a 64-bit Windows machine with a 13th Gen Intel® Core™ i9-13900 processor at 2.00 GHz and 64.0 GiB of RAM. With a discretization rate of 30 Hz and 29 spatial points, the algorithm achieved a real-time factor of 1.52 ± 0.33, demonstrating its feasibility for real-time feedback control.

IV. Conclusion

We reported a dynamic state estimation algorithm for continuum robots. It was able to recover all infinite-dimensional robot states by measuring the internal wrench at the robot's base using embedded F/T sensors. By combining dual boundary corrections, the observers achieved faster convergence and improved accuracy in the presence of perturbations and modeling errors. These conclusions were validated using experimental data from a tendon-driven continuum robot. Our future work is to use the algorithms for feedback control.

References

[1] S. Song, Z. Li, H. Yu, and H. Ren, "Electromagnetic positioning for tip tracking and shape sensing of flexible robots," *IEEE Sensors Journal*, vol. 15, no. 8, pp. 4565–4575, 2015.

[2] H. Bezawada, C. Woods, and V. Vikas, "Shape estimation of soft manipulators using piecewise continuous pythagorean-hodograph curves," in *American Control Conference*, 2022, pp. 2905–2910.

[3] P. L. Anderson, A. W. Mahoney, and R. J. Webster, "Continuum reconfigurable parallel robots for surgery: Shape sensing and state estimation with uncertainty," *IEEE Robotics and Automation Letters*, vol. 2, no. 3, pp. 1617–1624, 2017.

[4] S. Lilge, T. D. Barfoot, and J. Burgner-Kahrs, "Continuum robot state estimation using gaussian process regression on se(3)," *The International Journal of Robotics Research*, vol. 41, no. 13-14, pp. 1099–1120, 2022.

[5] J. C. Simo and L. Vu-Quoc, "On the dynamics in space of rods undergoing large motions—a geometrically exact approach," *Computer methods in applied mechanics and engineering*, vol. 66, no. 2, pp. 125–161, 1988.

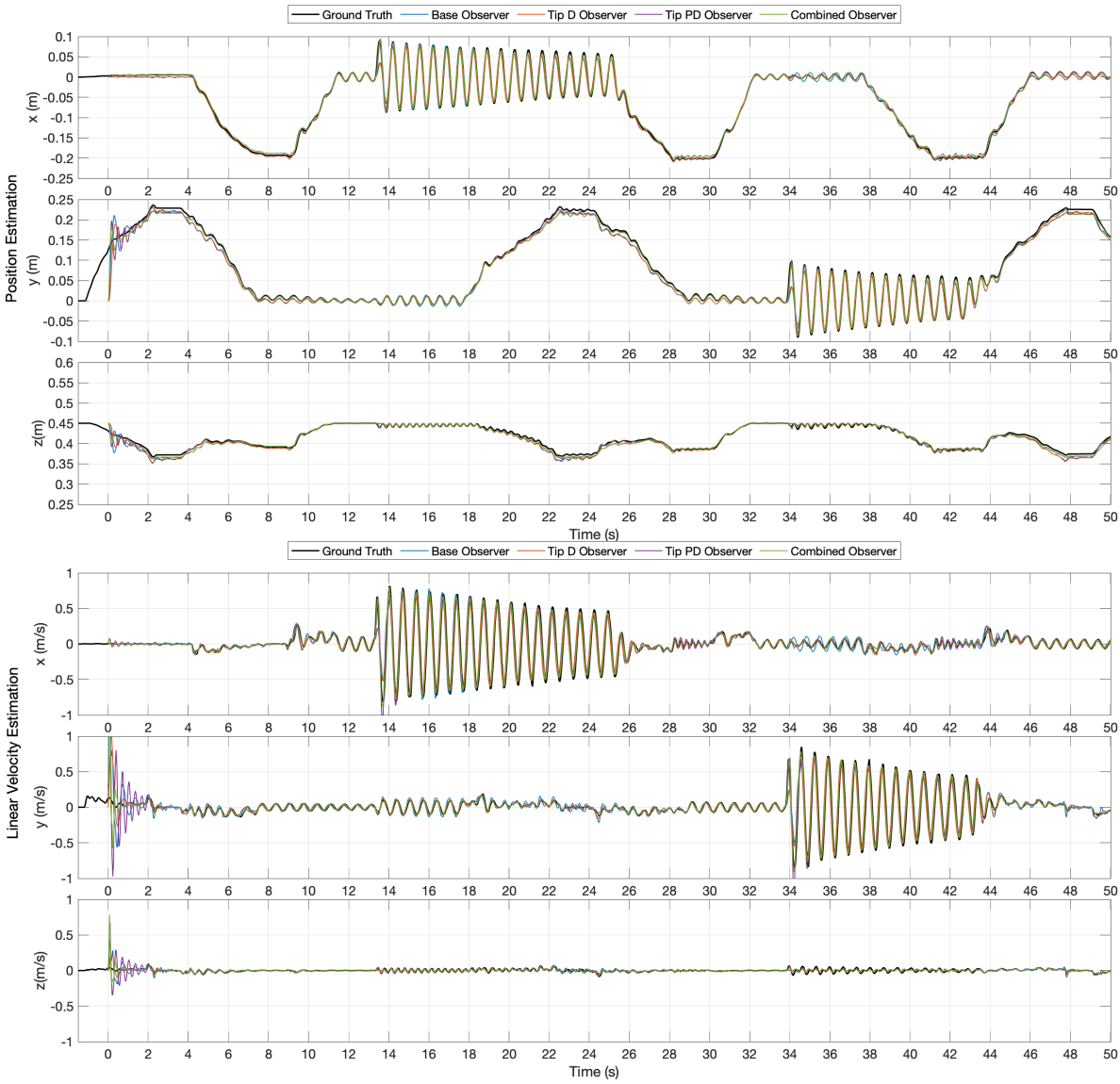

Fig. 3. This figure presents a comparison between the ground truth and estimated position and linear velocity at the three-quarter point of the robot. The estimation algorithms were initialized while the robot was already in motion. All observers converged to the ground truth within 3 seconds with steady-state errors. The tip PD and combined observers demonstrated smaller steady-state errors. The base and tip D observers exhibited temporary deviations at $t = 13.5$ and 34 seconds due to unknown perturbations and re-converged within 1 second. The tip PD and combined observers still tracked the ground truth even in the presence of unknown perturbations. The combined observer demonstrated the fastest convergence and the minimum oscillations.

[6] D. C. Rucker and R. J. Webster III, "Statics and dynamics of continuum robots with general tendon routing and external loading," *IEEE Transactions on Robotics*, vol. 27, no. 6, pp. 1033–1044, 2011.

[7] F. Renda, M. Giorelli, M. Calisti, M. Cianchetti, and C. Laschi, "Dynamic model of a multibending soft robot arm driven by cables," *IEEE Transactions on Robotics*, vol. 30, no. 5, pp. 1109–1122, 2014.

[8] C. Rucker, E. J. Barth, J. Gaston, and J. C. Gallentine, "Task-space control of continuum robots using underactuated discrete rod models," in *2022 IEEE/RSJ International Conference on Intelligent Robots and Systems (IROS)*. IEEE, 2022, pp. 10 967–10 974.

[9] C. Della Santina, R. K. Katzschmann, A. Bicchi, and D. Rus, "Model-based dynamic feedback control of a planar soft robot: trajectory tracking and interaction with the environment," *The International Journal of Robotics Research*, vol. 39, no. 4, pp. 490–513, 2020.

[10] F. Renda, F. Boyer, J. Dias, and L. Seneviratne, "Discrete cosserat approach for multisection soft manipulator dynamics," *IEEE Transactions on Robotics*, vol. 34, no. 6, pp. 1518–1533, 2018.

[11] F. Boyer, V. Lebastard, F. Candelier, and F. Renda, "Dynamics of continuum and soft robots: A strain parameterization based approach," *IEEE Transactions on Robotics*, vol. 37, no. 3, pp. 847–863, 2020.

[12] J. Y. Loo, C. P. Tan, and S. G. Nurzaman, "H-infinity based extended kalman filter for state estimation in highly non-linear soft robotic system," in *American Control Conference*, 2019, pp. 5154–5160.

[13] K. Stewart, Z. Qiao, and W. Zhang, "State estimation and control with a robust extended kalman filter for a fabric soft robot," *IFAC-PapersOnLine*, vol. 55, no. 37, pp. 25–30, 2022.

[14] D. Feliu-Talegon, A. T. Mathew, A. Y. Alkayas, Y. A. Adamu, and F. Renda, "Dynamic Shape Estimation of Tendon-Driven Soft Manipulators via Actuation Readings," *IEEE ROBOTICS AND AUTOMATION LETTERS*, vol. 10, no. 1, 2025.

[15] T. Zheng, C. McFarland, M. Coad, and H. Lin, "Estimating infinite-dimensional continuum robot states from the tip," in *IEEE International Conference on Soft Robotics*, 2024, pp. 572–578.

[16] T. Zheng, Q. Han, and H. Lin, "Full state estimation of continuum robots from tip velocities: A cosserat-theoretic boundary observer," *IEEE Transactions on Automatic Control (to appear)*, 2025.

[17] F. Renda, C. Armanini, V. Lebastard, F. Candelier, and F. Boyer, "A geometric variable-strain approach for static modeling of soft manipulators with tendon and fluidic actuation," *IEEE Robotics and Automation Letters*, vol. 5, no. 3, pp. 4006–4013, 2020.